Drop Formation in Liquid-liquid Systems from Single Nozzles

HAROLD R. NULL and HOMER F. JOHNSON

University of Tennessee, Knoxville, Tennessee

Interfacial area is an important variable in mass transfer operations. In liquid-liquid extraction systems, where interfacial area comprises drop surfaces, the area can be computed if drop sizes are known. This work presents a new correlation which predicts volumes of drops formed from single nozzles to within 20% throughout the range of nozzle flow rates for which uniform drop sizes are obtained.

For years it has been the practice of experimenters in the field of liquid-liquid extraction to evaluate their data in terms of the product of the over-all mass transfer coefficient and the interfacial area available for mass transfer per unit volume of tower. Although the need for a basis by which to determine these two parameters separately has been recognized, the means for doing so have in most instances not been available.

In the case of a spray tower the area available for mass transfer is directly proportional to the average surface area of the individual drops, which, in turn, is a function of the volume and shape of the drops. A method of predicting static drop sizes is well established by the work of Harkins and Brown (*2, 3*), and a study has been made by Hayworth and Treybal (*4*) on the prediction of drop volumes for various flow rates of a dispersed phase into a static continuous phase from a single nozzle. This study was the logical first step toward predicting the interfacial area available for extraction, but Batson (*1*) was unable to verify the correlation obtained by Hayworth and Treybal. Batson found that for the system he studied, methyl isobutyl ketone dispersed in water, the drop volumes were all smaller than predicted and that two points of relative maximum were obtained when drop size was plotted vs. flow rate; whereas the correlation of Hayworth and Treybal gave only one maximum. Null (*6*) later obtained results in agreement with Batson, and the need for a more reliable method of predicting drop volumes from a single nozzle was established. It is the purpose of this paper to present a basic model for drop formation from single nozzles which may be used as the starting point in further search for a general method of predicting the interfacial area available in extraction towers.

H. R. Null is now associated with the University of Dayton, Dayton, Ohio.

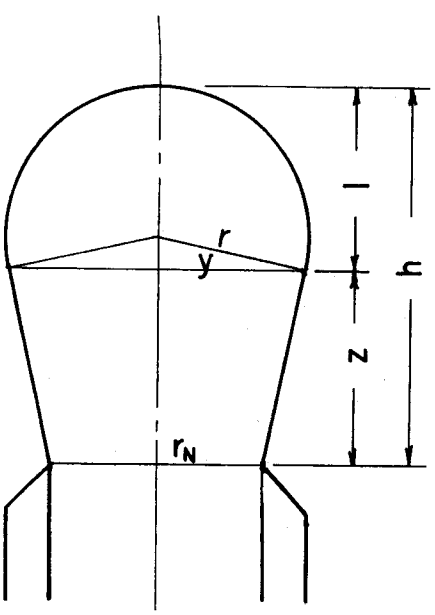

Fig. 1. Geometry of drop before break.

THEORY

The theoretical treatment of the drop-formation phenomenon is primarily one of geometry. The assumptions used are, for the most part, suggested by actual observation of drops with the aid of

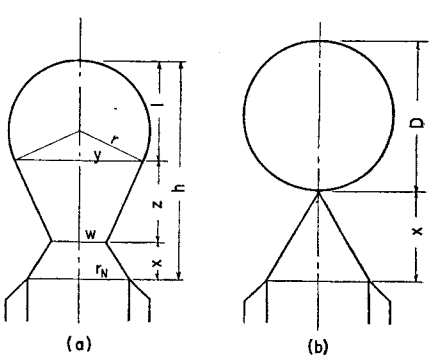

Fig. 2. Drop geometry during break period.

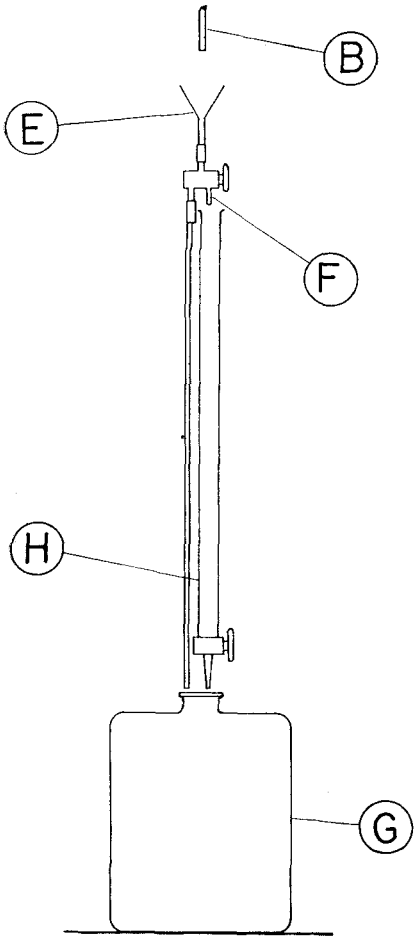

Fig. 3. Apparatus for flow measurement.

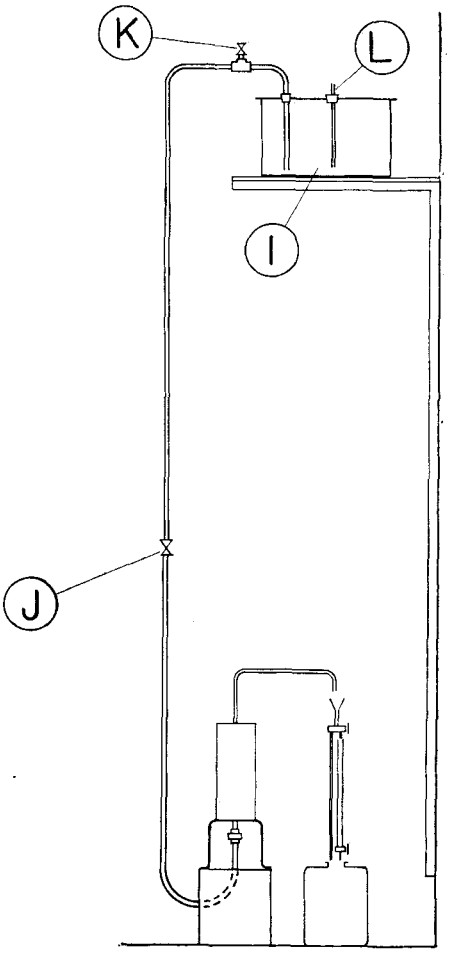

Fig. 4. Drop-dispersing apparatus.

stroboscopic light. Two distinct phases of the drop formation will be considered—the period of time during which the drop is growing but has not begun to break away from the nozzle and the period of time during which the process of breaking away is actually occurring. A more detailed treatment of the theory may be found in reference 5.

The model adopted for the period of drop growth before breaking is that of a sphere atop, and tangent to, a right-truncated cone passing through the circumference of the nozzle. This model and its dimensions are shown in Figure 1. The drop is assumed to grow with leading-edge velocity v constant. It will also be assumed that throughout this initial period the dimension l constantly increases. Eventually the assumption of constant v will no longer be compatible with increasing l; i.e., l will have reached a maximum characterized by $dl/dt = 0$,

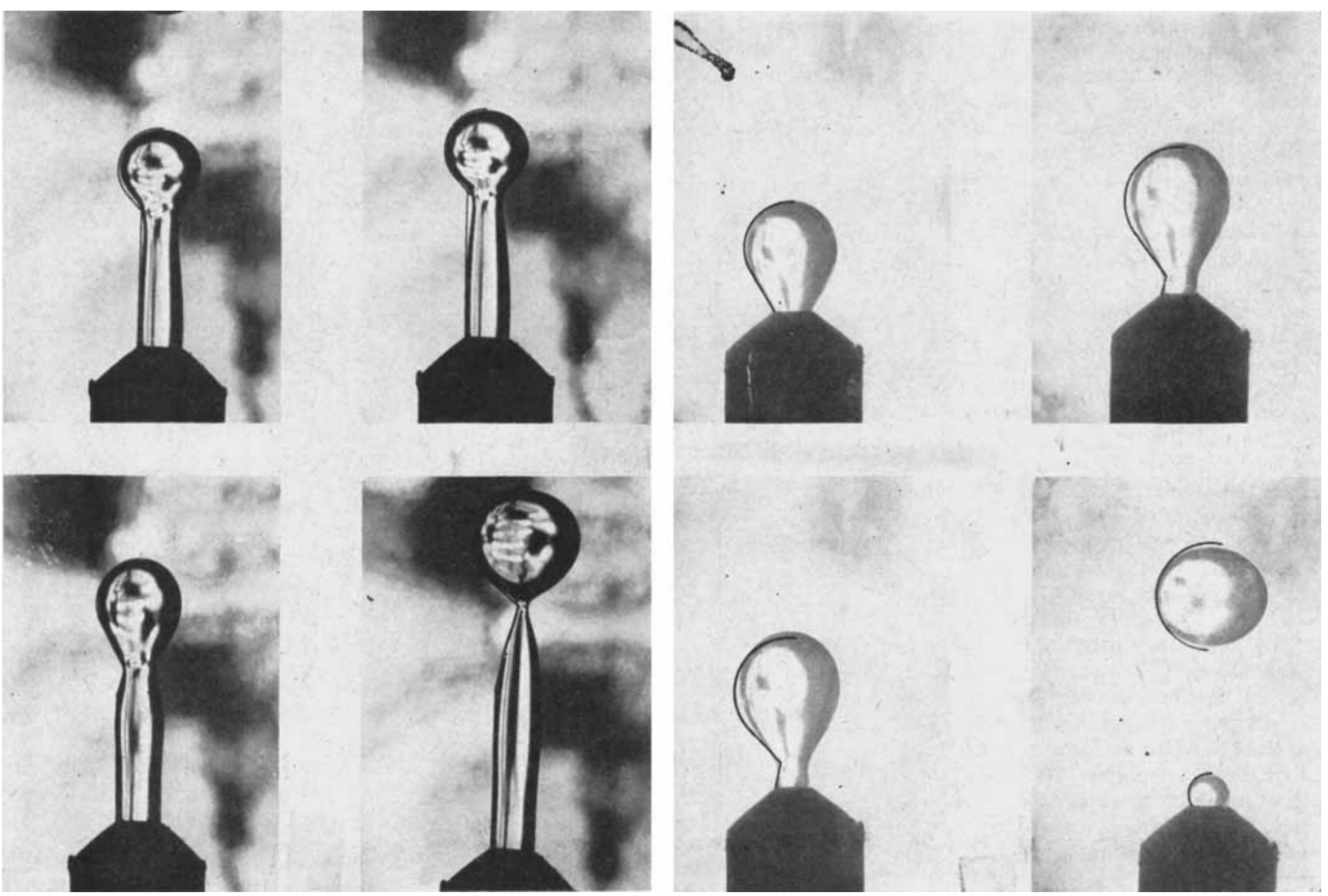

Fig. 5. Photographs of drop formation.
(a) Cottonseed oil dispersed in water. D_N = 0.314 cm., V_N = 0.764 cc./sec.;
(b) Cottonseed oil dispersed in water. D_N = 0.263 cm., V_N = 0.0438 cc./sec.

5a 5b

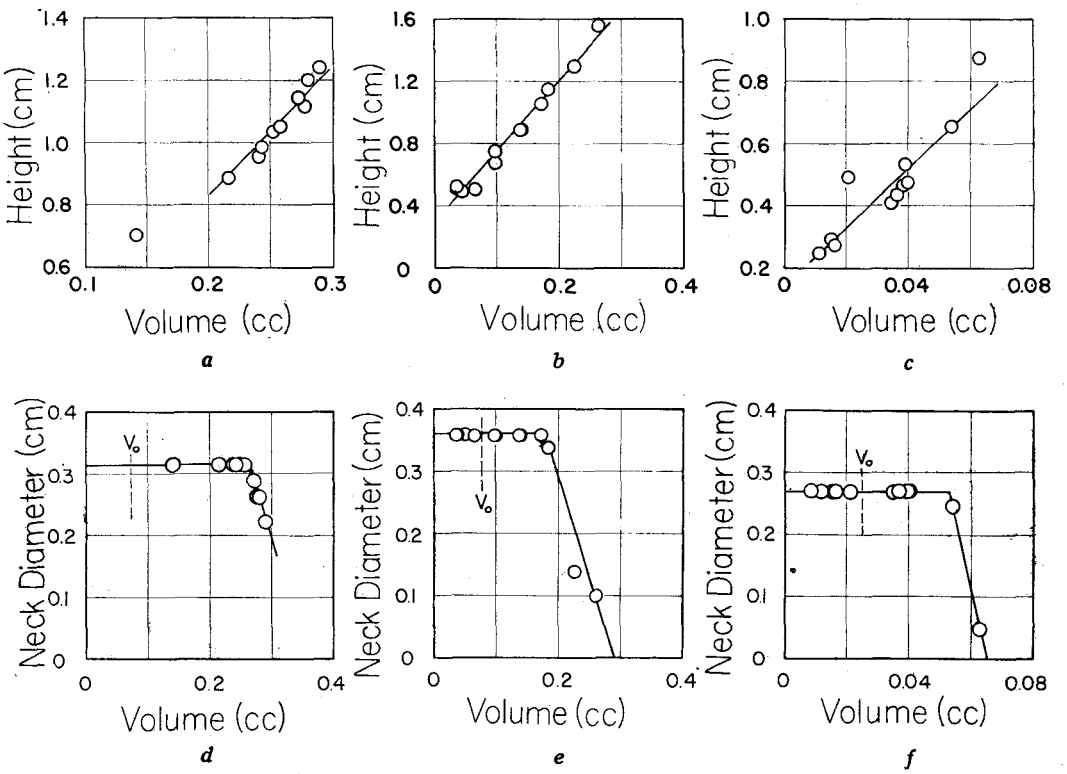

Fig. 6. Variation of drop dimensions.

a. Cottonseed oil in water.
b. Water in benzene.
c. Water in CCl_4.
d. Cottonseed oil in water.
e. Water in benzene.
f. Water in CCl_4.

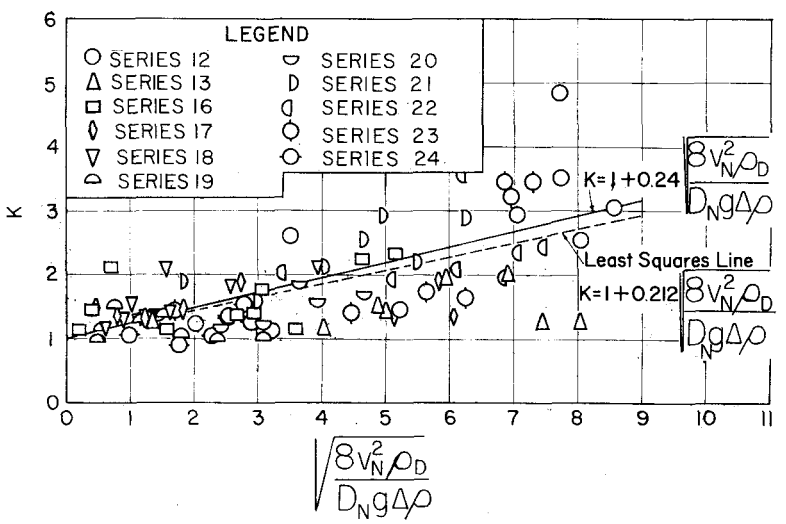

Fig. 7. Correlation of values of K.

when the period of simple drop growth will be assumed to end and the period of drop break away to begin. The geometry of the system coupled with constant flow rate and the condition $dl/dt = 0$ results in the following equation:

$$\frac{v}{v_N} = \frac{6(\beta^2 - 2\alpha^2\beta + \alpha^2)}{\beta^5 - \alpha^2\beta^3 + 2\beta^2 - 3\alpha^4\beta + 2\alpha^2} \quad (1)$$

and

$$\gamma = \frac{2\alpha\beta(\beta - 1)}{\alpha^2 - \beta^2} \text{ (from geometry)}$$

Equation (1) is valid whether v is considered constant or variable. The condition that v be constant leads to a condition that

$$\left.\frac{\partial\left(\frac{v}{v_N}\right)}{\partial y}\right]_0 = 0,$$

which in turn leads to the equation

$$3\beta^5 + (3\alpha - 8\alpha^2)\beta^4 + (6\alpha^2 - 8\alpha^3)\beta^3 + 6\alpha^3\beta^2 + (3\alpha^4 - 4\alpha^2)\beta + (3\alpha^5 - 4\alpha^3) = 0 \quad (2)$$

Equations (1) and (2) are sufficient to define α and β provided the value of v/v_N is known. The equations apply without modification to the cases $\alpha > 1$, $1 < \beta < \alpha$; $0 < \alpha < 1$, $\alpha < \beta < 1$; and $\alpha = \beta = 1$, which imply that the spherical segment in Figure 1 is respectively greater than, less than, and equal to a hemisphere. The volume of the drop at the beginning of the break V_o can be evaluated from geometric considerations which lead to

$$\frac{3V_o}{4\pi r_N^3} = \frac{\alpha}{8}(\alpha^2 + 3\beta^2) + \frac{\alpha}{4}(1 + \beta + \beta^2) \quad (3)$$

From the instant that the break begins until it is complete the configuration shown in Figure 2*a* is assumed with the limiting case for final break-away being as shown in Figure 2*b*. At this point it is necessary to define distinctly the terms *drop* and *jet* used in this discussion. During the break period the term drop is used to represent that portion of the fluid outside the nozzle but more remote from it than the distance x. The truncated cone having bases r_N and w is referred to as the jet. V designates the volume of the drop.

The total volume V_τ represented in Figure 2*a* consists of the volume of the drop V, plus the volume of the jet:

$$V_\tau = V + \frac{\pi}{3} \times (r_N^2 + r_N w + w^2) \quad (4)$$

and

$$x = h_0 + vt - l - z \quad (5)$$

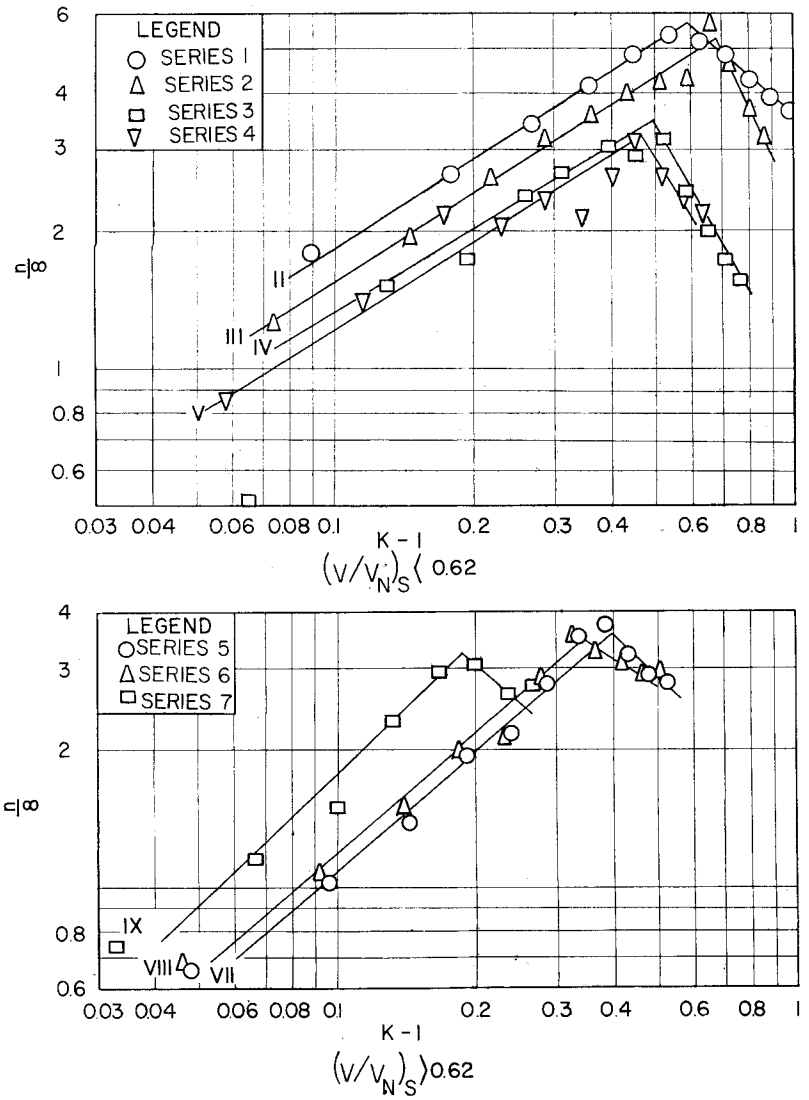

Fig. 8. Correlation of $n/8$ for the system methyl isobutyl ketone–water.

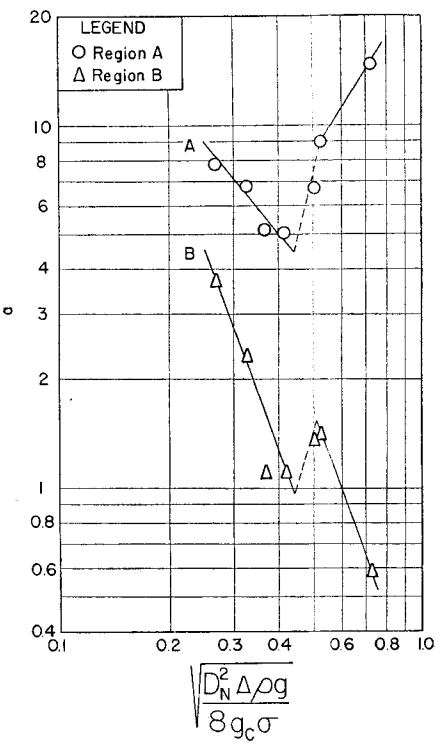

Fig. 9. Correlation of a of Equation (12).

Table 1. Summary of Conditions of Different Series

Series	Table number of ref. 5	Dispersed phase*	Continuous phase	ρ_c, g./cc.	ρ_D, g./cc.	σ, dynes/cm.	D_N, cm.	$\sqrt{\frac{D_N^2 \Delta\rho g}{8 g_c \sigma}}$
1	II	MIK	Water	0.9984	0.8039	9.48	0.1691	0.269
2	III	MIK	Water	0.9982	0.8025	9.58	0.2071	0.326
3	IV	MIK	Water	1.0040	0.8014	9.52	0.2475	0.396
4	V	MIK	Water	1.0000	0.8022	9.56	0.261	0.416
5	VII	MIK	Water	1.0000	0.8040	9.21	0.3115	0.503
6	VIII	MIK	Water	0.9988	0.8015	9.67	0.3307	0.523
7	IX	MIK	Water	0.9983	0.7994	9.85	0.460	0.724
8	X	Benzene	Water	1.0000	0.8707	29.66	0.460	0.341
9	XI	Benzene	Water	0.9981	0.8694	26.89	0.3307	0.253
10	XII	Benzene	Water	0.9994	0.8691	30.4	0.3115	0.226
11	XIII	Benzene	Water	0.9982	0.8693	30.2	0.261	0.193
12	XV	Benzene	Water	0.9992	0.8646	31.6	0.201	1.1469
13	XVI	Benzene	Water	0.9972	0.8639	28.9	0.252	0.1891
14	XVII	EA	Water	0.9969	0.8884	4.5	0.269	0.462
15	XVIII	EA	Water	0.9966	0.8891	4.13	0.305	0.545
16	XIX	CSO	Water	0.9978	0.9113	24.2	0.314	0.208
17	XX	CSO	Water	0.9973	0.9099	23.8	0.263	0.176
18	XXI	Water	CTC	1.5728	0.9970	31.5	0.270	0.376
19	XXII	Water	CTC	1.5783	0.9993	33.8	0.348	0.504
20	XXIII	CTC	Water	0.9911	1.5808	19.21	0.280	0.405
21	XXIV	Water	Benzene	0.8710	0.9969	28.5	0.358	0.235
22	XXV	Water	Benzene	0.8693	1.0015	29.8	0.260	0.192
23	XXVI	Water	CSO	0.9110	0.9987	25.6	0.260	0.168
24	XXVII	Water	CSO	0.9110	0.9987	25.6	0.358	0.232

*Abbreviations: MIK = methyl isobutyl-ketone, EA = ethyl acetate, CSO = cottonseed oil, CTC = carbon tetrachloride.

where t is the time from the beginning of the break. When Equation (4) is differentiated with respect to time, the flow rate results. If the result is evaluated at the instant represented by Figure 2*b*, at which time drop growth ceases, the assumption $dV/dt = 0$ seems reasonable. When the differentiation is performed and evaluated at the completion of the break, and Equation (5) is substituted therein, the result simplifies to:

$$r_N^2 v_N = \tfrac{1}{3}(h_0 + vt_f - l - z)(r_N + 2w)\frac{dw}{dt} + \tfrac{1}{3}(r_N^2 + r_N w + w^2)\left(v - \frac{dl}{dt} - \frac{dz}{dt}\right) \quad (6)$$

where t_f is the time at the completion of the break.

Equation (6) may be simplified by first observing that $l = D$, the final drop diameter, at $t = t_f$, and applying two further assumptions, namely that z varies with time by

$$z = z_0\left[1 - \left(\frac{t}{t_f}\right)^n\right] \quad (7)$$

and w varies linearly with time:

$$w = r_N\left(1 - \frac{t}{t_f}\right) \quad (8)$$

These assumptions lead to

$$\left.\frac{dz}{dt}\right]_{t=t_f} = -\frac{nz_0}{t_f}$$

$$\left.\frac{dw}{dt}\right]_{t=t_f} = -\frac{r_N}{t_f} \quad \text{and}$$

$$\left.\frac{dl}{dt}\right]_{t=t_f} = \frac{nz_0}{2t_f}$$

The foregoing assumption can be used to reduce Equation (6) to

$$t_f = \frac{(D - h_0) + \frac{nz_0}{2}}{3v_N} \qquad (9)$$

There is still another relation available for determining t_f. If F denotes the frequency of drop formation,

$$\frac{1}{F} = \frac{D^3}{6r_N^2 v_N}$$

is the total time required for the drop to form and is equal to t_f plus the time required for the volume of the drop to increase from the jet volume of Figure 2*b* to the volume V_0 when the next drop begins to break away, or

$$\frac{D^3}{6r_N^2 v_N} = \frac{V_0 - \frac{\pi}{3}(h_0 + vt_f - D)r_N^2}{\pi r_N^2 v_N} + t_f \qquad (10)$$

Equations (9) and (10) combine to give

$$\left(\frac{D}{D_N}\right)^3 - A\left(\frac{D}{D_N}\right) - \left(B + \frac{n}{8}C\right) = 0 \qquad (11)$$

where

$$A = \frac{1}{2}\left(2 - \frac{1}{3}\frac{v}{v_N}\right)$$

$$B = \frac{3V_0}{4\pi r_N^3} - \frac{1}{4}\left(2 - \frac{1}{3}\frac{v}{v_N}\right)(\alpha + \gamma)$$

and

$$C = \gamma\left(1 - \frac{1}{3}\frac{v}{v_N}\right)$$

Equation (11), together with Equations (1), (2), (3), and the expression for γ, affords a means of computing drop sizes from a knowledge of only v/v_N and n.

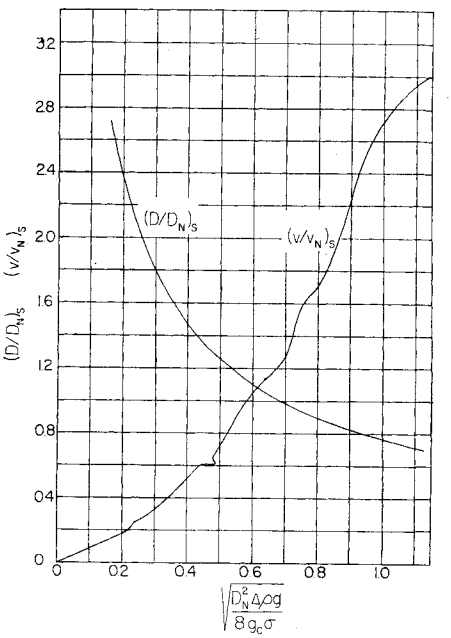

Fig. 10. Static drop parameters.

The simplest possible behavior for n would be for it to be zero for zero flow rate of dispersed phase and have a positive value for positive flow rates. It was observed in the theoretical portion of this work that v/v_N for positive dispersed phase flow rate is always greater than for static drop formation, or

$$K \equiv \left(\frac{v}{v_N}\right) \Big/ \left(\frac{v}{v_N}\right)_s \geq 1$$

where the subscript s designates static conditions. A simple form which suggests itself, then, is

$$\frac{n}{8} = a(K - 1)^b \qquad (12)$$

where a and b are to be determined experimentally. Equation (11) gives, for the static case,

$$\left(\frac{D}{D_N}\right)_s^3 - A_s\left(\frac{D}{D_N}\right)_s - B_s = 0 \qquad (13)$$

and since $(D/D_N)_s$ can be determined from the work of Harkins and Brown (*2, 3*) where the correction factor to Tate's law is given as function of $\sqrt{D_N^2\Delta\rho g/8\sigma g_c}$, Equation (13) is seen to relate $(v/v_N)_s$ to $\sqrt{D_N^2\Delta\rho g/8\sigma g_c}$.

The factors which influence the value of v/v_N are now to be further investigated. As indicated in Figure 2*b*, the vertex of the cone forming the jet will become the leading edge of the succeeding drop. If the point does not retract, the distance travelled by the leading edge of a drop during formation v/F is equal to D, the final drop diameter, or $v/FD = 1$. Actually, the point does retract, being supported by the impact force, P_I, and the buoyant force, P_B, and retracted by the surface tension P_T. Dimensional analysis of these factors results in

$$\frac{v}{FD} = \Phi\left(\frac{P_I}{P_T}, \frac{P_B}{P_T}\right)$$

which can lead to

$$K = f\left(\sqrt{\frac{D_N^2\Delta\rho g}{8g_c\sigma}}, \sqrt{\frac{D_N v_N^2 \rho_D}{g_c\sigma}}\right) \qquad (14)$$

Evaluation of a and b of Equation (12) and determination of the form of f in Equation (14) are to be done experimentally.

The theoretical treatment has assumed a case of the drop forming at the top of the nozzle. Actually, the approach is also extended to the case where an extended jet appears at the nozzle by merely considering the jet as a cylinder of liquid with a cone at its end and considering the model developed herein as occurring at the end of the cylindrical portion of the jet. This model then becomes equivalent to the case illustrated in Figures 1 and 2.

APPARATUS AND PROCEDURE

The apparatus used for the experimental portion of the work is shown in Figures 3 and 4. The apparatus consisted of a square, stainless-steel column having two sides made of plate glass. The dispersed phase was admitted into the column through a nozzle and withdrawn through a tube at the other end. A drain was provided for the column. The holder for the nozzle was tapped to accommodate the ¼-in. feed line on the upstream side and the ⅛-in. pipe threads of the nozzle on the downstream side. Each nozzle consisted of a two-inch length of ⅜-in. rod through which the hole was drilled. One end was threaded with ⅛-in. pipe threads to fit the holder; the other end was chamferred away from the opening at a 45° angle to prevent spreading of the dispersed phase onto the metal around the opening. All nozzles were constructed of stainless steel or aluminum. Altogether sixteen inside nozzle diameters varying from 0.1691 to 0.460 cm. were studied. The discharge from tube B was directed into a funnel E (Figure 3) connected to a three-way stop cock, F which could be used to collect the dispersed phase in a burette H or a waste bottle G. Dispersed-phase

Table 2. Sample Experimental Data from Series 13.

Run	Dispersed-phase flow rate, cc./sec.	V, cc.	$\sqrt{\frac{D_N v_N^2 \rho_D}{g_c\sigma}}$	$\frac{6V}{\pi D_N^3}$	v, cm./sec.	$\frac{v}{v_N}$	K	$\sqrt{\frac{8v_N^2\rho_D}{D_N g\Delta\rho}}$
1	0.1472	0.1738	0.248	20.7	0.589	0.206	1.226	1.31
2	0.437	0.1683	0.763	20.1	2.17	0.190	1.131	4.03
3	0.646	0.1343	1.128	16.02	4.15	0.320	1.902	5.96
4	0.531	0.1518	0.925	18.10	2.70	0.253	1.502	4.89

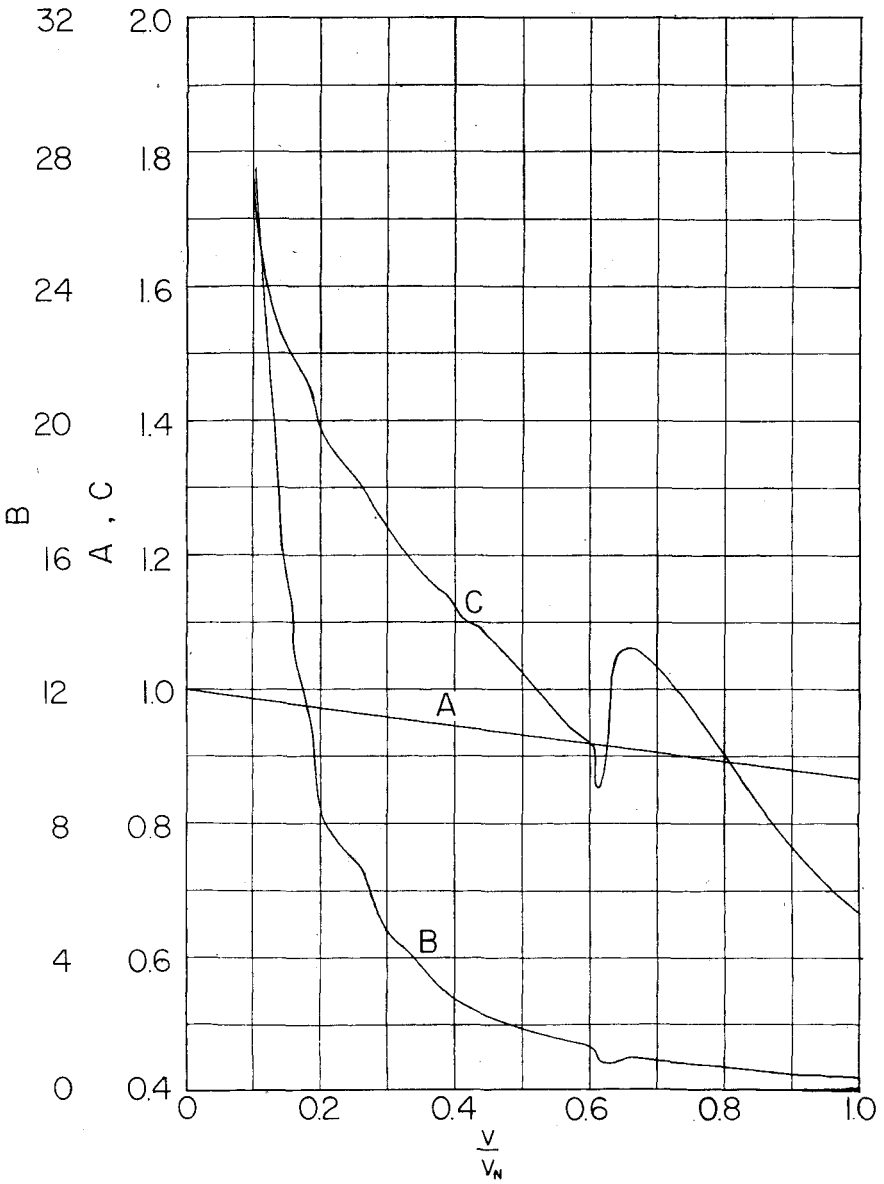

Fig. 11*a*. Coefficients of drop-volume equation.

flow was controlled by a needle valve *J* (Figure 4). The dispersed-phase head tank *I* was closed and equipped with a tube *L* to assure constant pressure of 1 atm. at the lower end of the tube. A valve *K*, was provided to bleed air out of the feed line.

Before a series of runs was made, the head tank was filled with the phase to be dispersed plus a layer of the continuous phase to maintain mutual saturation, and the column was filled with continuous phase containing a layer of the dispersed phase. This was normally done the day before the run was to be made. For a typical run the flow rate was adjusted and allowed to reach steady state. The frequency of the drop formation was then determined by adjusting a strobotac until the drop image at the nozzle tip appeared stationary. The dispersed-phase overflow was then directed into the burette for a period of time measured by a stopwatch to determine the flow rate. Photographs were then taken of the drop as it formed, after which a new flow setting was made. The photographs were taken with the aid of a strobolux acting as slave to the strobotac or with a strobolume as a single flash source. In either case the light source was shown through the column into the lens of the camera, an Exakta VX. For the earlier runs, an attempt was made to capture the drop image at the exact break-away instant, but when it later became apparent that a determination of drop front velocity during formation was important, several photographs were taken at each flow setting. From these photographs the height of the drop was measured directly and time was determined by graphical integration of the contour of the liquid outside the nozzle to determine total volume, which was in turn proportional to time. The accuracy of the graphical integration was found to be ±3% by comparing the volume found by integrating the outline of completely formed drops, such as appear in Figure 5*b*, with the volume determined by frequency and flow rate measurements. The average deviation from the lines determining frontal velocity v was not determined, but scatter was slight, as indicated in Figure 6*a*, *b*, and *c*. The results are based on the data of the systems and conditions enumerated in Table 1. Table 2 gives an example of the data obtained from one series of runs.

The density of each phase was measured at the end of each series of runs with a Westphal chain balance, and the interfacial tension was measured with a du Nuoy Tensiometer. The value of 19.21 dynes/cm. for the carbon tetrachloride-water system of Series 20 is abnormally low. This is believed to be due to contamination by the gasket material of the head tank; subsequently carbon tetrachloride was not used as dispersed phase.

RESULTS

Drop Appearance

The theoretical model adopted was based upon the actual appearance of the drop image observed by the authors. Figure 5 shows photographs of drops during various stages of formation with the assumed configuration superimposed. These photographs are typical of photographs of all systems and indicate the validity of the configuration assumed for the theoretical treatment. Complete original and calculated data are reported in reference *5*.

Test of Assumptions

Figure 6 contains typical plots of leading edge height and neck radius as a function of total volume of dispersed phase outside the nozzle. Since for constant flow rate the total volume outside the nozzle is proportional to time, linearity of these plots indicates linearity with time. Constant leading edge velocity is indicated by Figures 6*a*, 6*b*, and 6*c*, although Figures 6*d*, 6*e*, and 6*f* leave considerable doubt as to the validity of the assumption of linearity of neck radius with time. The plots of neck diameter against total volume also have indicated on them values of V_0 for the runs from which the data were taken. Since the values of V_0 do not include the volumes of the extended jets, such as is shown in Figure 5*a*, V_0 should always be equal to or less than the total volume outside the nozzle at the beginning of the break period. This was universally true for all

values of V_0, and the greatest deviation from equality occurred in those systems exhibiting the longest extended jets.

Evaluation of Empirical Functions

When each set of data was taken individually, K was found to vary linearly with $\sqrt{D_N v_N^2 \rho_D / g_c \sigma}$, and the slopes of these plots varied inversely with $\sqrt{D_N^2 \Delta\rho g / 8 g_c \sigma}$. The resulting equation is

$$K = 1 + 0.24 \sqrt{\frac{8 v_N^2 \rho_D}{D_N g \Delta\rho}} \qquad (15)$$

where $\sqrt{8 v_N^2 \rho_D / D_N g \Delta\rho}$ is the ratio of the two dimensionless groups $\sqrt{D_N v_N^2 \rho_D / g_c \sigma}$ and $\sqrt{D_N^2 \Delta\rho g / 8 g_c \sigma}$. The combined plot of all the leading edge velocity data is shown in Figure 7 with the exception of the ethyl acetate-water system. This system is omitted because the two liquids involved are sufficiently soluble so that mutual saturation was never obtained. Therefore, some mass transfer occurred during drop formation, and the appropriate value of the interfacial tension was not known.

The data from which $n/8$ could be computed directly scattered too much for a and b of Equation (12) to be determined; a small error in v/v_N results in a large error in both γ and $3V_0/4\pi r_N^3$, and thus considerable precision in the measurement of v/v_N would be required. Therefore, in order to obtain a correlation for $n/8$, the smoothed curves representing the experimental drop size data for the system methyl-isobutyl ketone dispersed in water were used in Equation (11) to determine $n/8$. Equation (15) was employed to determine v/v_N and K. Values of $n/8$ and K thus obtained are plotted in Figure 8. The value of a versus $\sqrt{D_N^2 \Delta\rho g / 8 g_c \sigma}$ is shown in Figure 9, and the final correlation obtained is shown below

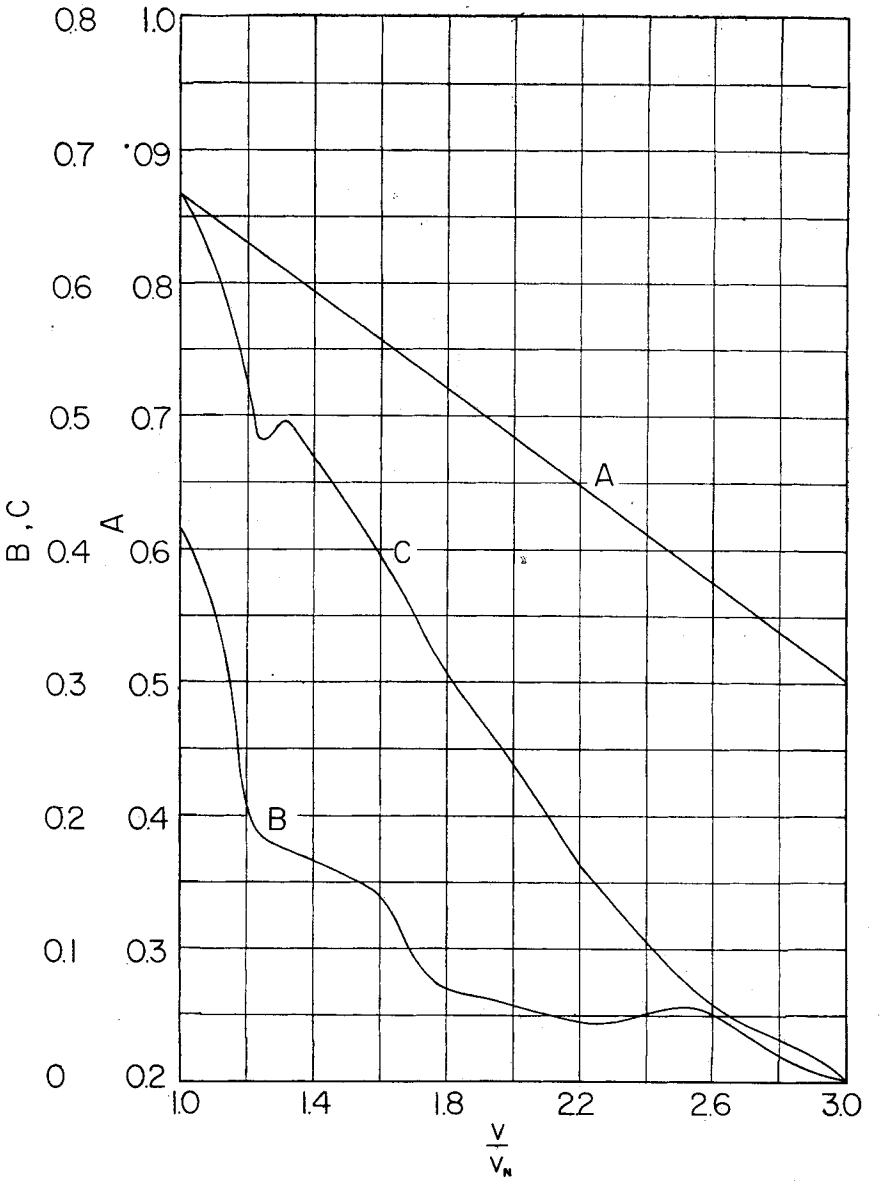

Fig. 11*b*. Coefficients of drop-volume equation.

For $\left(\frac{v}{v_N}\right)_s < 0.62$, or $\sqrt{\frac{D_N^2 \Delta\rho g}{8 g_c \sigma}} < 0.49$

$$\left.\begin{aligned} \text{A}\quad \frac{n}{8} &= 1.85\left(\sqrt{\frac{D_N^2 \Delta\rho g}{8 g_c \sigma}}\right)^{-1.15} (K-1)^{\frac{3}{4}}, \quad K \le 1 + 0.25\left(\sqrt{\frac{D_N^2 \Delta\rho g}{8 g_c \sigma}}\right)^{-0.807} \\ \text{B}\quad \frac{n}{8} &= 0.092\left(\sqrt{\frac{D_N^2 \Delta\rho g}{8 g_c \sigma}}\right)^{-2.9} (K-1)^{-\frac{3}{4}}, \quad K \ge 1 + 0.25\left(\sqrt{\frac{D_N^2 \Delta\rho g}{8 g_c \sigma}}\right)^{-0.807} \end{aligned}\right\} \qquad (16)$$

For $\left(\frac{v}{v_N}\right)_s > 0.62$, or $\sqrt{\frac{D_N^2 \Delta\rho g}{8 g_c \sigma}} > 0.49$

$$\left.\begin{aligned} \text{A}\quad \frac{n}{8} &= 22.9\left(\sqrt{\frac{D_N^2 \Delta\rho g}{8 g_c \sigma}}\right)^{1.45} (K-1)^{0.9}, \quad K \le 1 + 0.108\left(\sqrt{\frac{D_N^2 \Delta\rho g}{8 g_c \sigma}}\right)^{-1.816} \\ \text{B}\quad \frac{n}{8} &= 0.334\left(\sqrt{\frac{D_N^2 \Delta\rho g}{8 g_c \sigma}}\right)^{-2.2} (K-1)^{-1}, \quad K \ge 1 + 0.108\left(\sqrt{\frac{D_N^2 \Delta\rho g}{8 g_c \sigma}}\right)^{-1.816} \end{aligned}\right\} \qquad (17)$$

Since Equations (16) and (17) do not coincide at $\sqrt{D_N^2 \Delta\rho g / 8 g_c \sigma} = 0.49$, a transition region is suggested, and the equations are not recommended for $0.47 \le \sqrt{D_N^2 \Delta\rho g / 8 g_c \sigma} \le 0.51$.

Computation of Drop Volumes

A series of charts, Figures 10 to 14, have been prepared to aid in the computation of drop sizes based on the results of the current investigation. The steps in computing drop sizes are as follows:

1. Given the properties of the system, find the value of $\sqrt{D_N^2 \Delta\rho g / 8 g_c \sigma}$. This determines the values of $(D/D_N)_s$ and of $(v/v_N)_s$, which may be found from Figure 10, prepared from the work of Harkins and Brown, and solutions of Equation (13).
2. Compute the value of

$$\sqrt{8 v_N^2 \rho_D / D_N g \Delta\rho}$$

This determines K by the equation

$$K = 1 + 0.24 \sqrt{\frac{8 v_N^2 \rho_D}{D_N g \Delta\rho}} \qquad (15)$$

3. Compute $v/v_N = (v/v_N)_s K$.
4. Find the values of A, B, and C from Figure 11*a* or 11*b* which were prepared by solution of Equations (1) and (2) and the definitions of A, B, and C.
5. Find values of $n/8$ from Figures 12 and 13 prepared from Equations (16) and (17).

6. Compute $(n/8)C$ and $(B + (n/8)C)$.

7. Use A and $(B + (n/8)\ C)$ to determine D/D_N from Figure 14*a* or 14*b*, which represents solutions of Equation (11).

8. The drop volume may now be computed from

$$V = \frac{\pi}{6} D_N{}^3 \left(\frac{D}{D_N}\right)^3$$

Accuracy of Correlations

The computation of drop volumes has been carried out for each system studied. Typical plots of actual drop volume and computed curve volumes are given in Figure 15. The average deviation of experimental from computed values of drop volume has been calculated by the method of this paper and by the method of Hayworth and Treybal (4). The results are shown in Table 3, which indicates a better correlation by the present method for all but three series. The deviations on a volume basis are approximately three times as great as they would be on a diameter basis, but it is felt that the volume basis should be used since the equivalent diameter is a derived quantity. The deviations are quite acceptable for all systems except ethyl acetate-water, for which the phases were known to be unsaturated. The over-all average deviation was 20% for all runs; 15.5% when the ethyl acetate-water system was omitted; 7.55% for methyl isobutyl ketone-water, for which most data were taken; and 18.46% for the benzene-water system, which was used most extensively by Hayworth and Treybal. On the same bases the Hayworth and Treybal correlation gave deviations of 87.4%, 72.2%, 73.1%, and 27.47% respectively.

CONCLUSIONS

A model has been proposed which does satisfactorily describe liquid-liquid drop formation and predict drop volumes for flow rates in the range of $0 \leq \sqrt{D_N v_N{}^2 \rho_D / g_c \sigma} \leq 1.4$. It may be possible to refine the description further to obtain a more accurate prediction of drop volume by means of modification of the various assumptions used in the present derivation, but the over-all approach appears generally applicable. For example, the correlation obtained for n is far from conclusive, and the assumption that the neck radius varies linearly with time is not conclusively verified by the data. The high values obtained for n, in fact, are much greater than normally expected for physical phenomena obeying the type of law assumed for the variation of z. The value of n, however, may be greatly reduced by assuming the neck radius to vary as the square of time rather than linearly, all of which suggests that the most important assumption to be investigated in refining the approach outlined herein is the linearity of neck radius with time.

Further investigation will be necessary before the approach outlined can be extended to multiple nozzles, as encountered in liquid-liquid extraction.

NOTATION

A = parameter of drop-diameter equation, equal to $\frac{1}{2}(2 - \frac{1}{3}(v/v_N))$

B = parameter of drop-diameter equation, equal to $3V_0/4\pi r_N{}^3$

$$-\frac{1}{4}\left(2 - \frac{1}{3}\frac{v}{v_N}\right)\frac{h_0}{r_N}$$

C = parameter of drop-diameter equation, equal to $\gamma(1 - \frac{1}{3}(v/v_N))$

D = diameter of drop during and after formation

D_N = inside diameter of nozzle

F = frequency of drop formation

K = ratio of true value of v/v_N to the static value, $(v/v_N)_s$

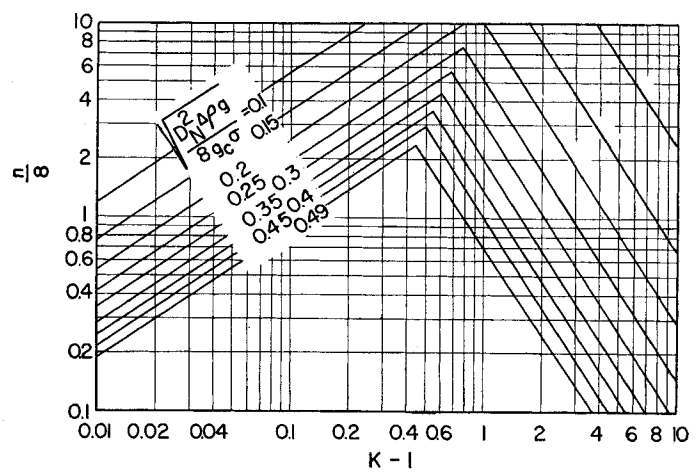

Fig. 12. Values of $n/8$ for $(v/v_N)_s < 0.62$.

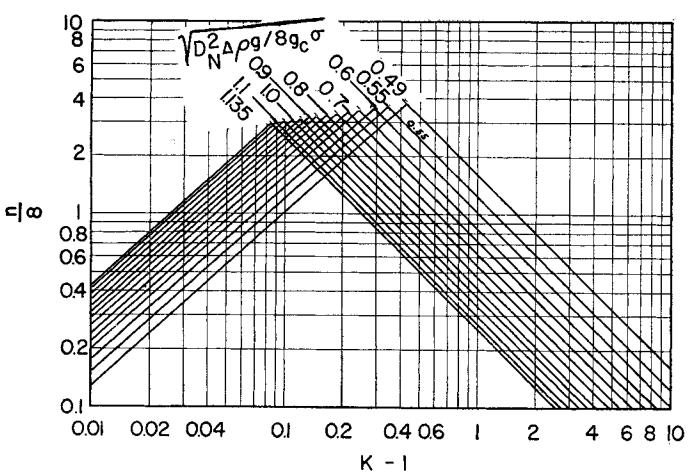

Fig. 13. Values of $n/8$ for $(v/v_N)_s > 0.62$.

Table 3. Deviations of Experimental from Calculated Drop Volumes

Series	Average percentage of deviation by proposed method	Average percentage of deviation from Hayworth and Treybal correlation
1	8.4	121.
2	5.0	94.
3	9.8	70.
4	7.5	65.
5	6.7	47.
6	6.8	37.5
7	7.5	28.8
8	16.7	18.0
9	30.5	9.5
10	12.2	28.4
11	11.4	20.2
12	21.6	61.
13	17.4	24.7
14	94.	377.
15	90.	325.
16	24.3	26.6
17	26.0	14.0
18	30.6	121.
19	22.3	130.
20	26.6	233.
21	14.6	53.
22	25.5	22.2
23	15.0	169.
24	55.	235.

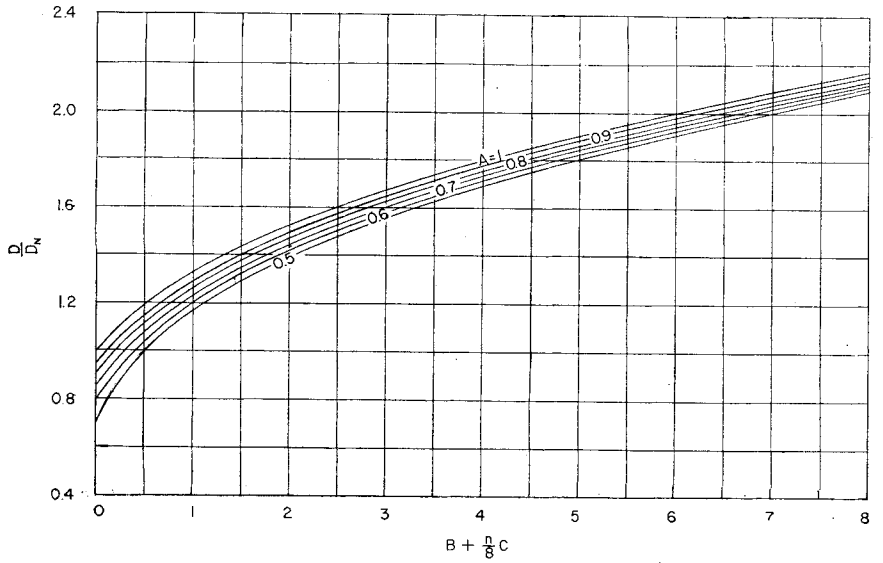

Fig. 14*a*. Solutions of drop-diameter equation.

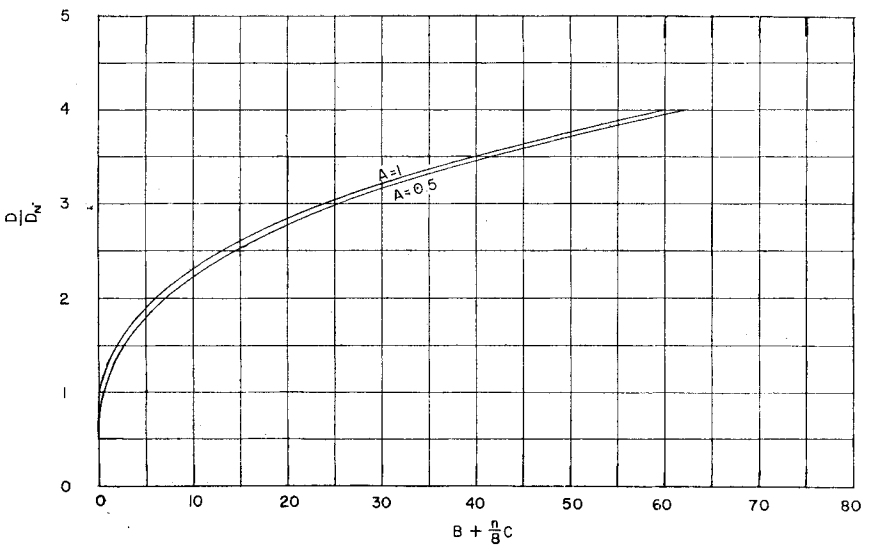

Fig. 14*b*. Solutions of drop-diameter equation.

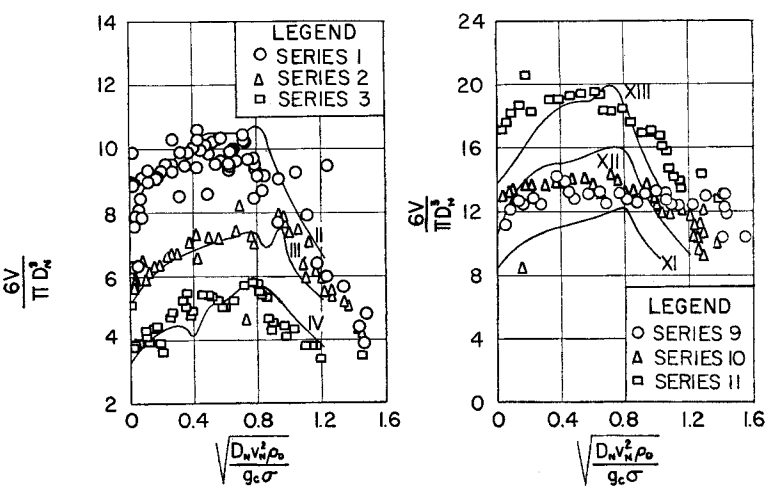

Fig. 15. Comparison of experimental data with theory.

P_B, P_I, P_T = buoyant, impact, and surface contraction forces on jet immediately after drop separation
V = volume of a drop during and after formation
V_N = volumetric flow rate of dispersed phase
V_s = drop volume for formation at zero dispersed phase flow rate
a = empirical constant
b = empirical constant
g = gravitational acceleration
g_c = conversion factor
h = distance from nozzle tip to leading edge of drop being formed
l = height of spherical segment portion of drop during formation
n = exponent representing the order of decrease of dimension z during drop break-away period
r = radius of spherical portion of the drop during formation
r_N = inside radius of nozzle
t = time
v = velocity of leading edge of drop during formation
v_N = velocity of dispersed phase flowing through the nozzle
w = radius of jet at its narrowest point during break-away period
x = height of jet during break-away period
y = radius of base of spherical-segment portion of drop during its formation
z = height of truncated-cone portion of drop during its formation

Greek Letters

α = dimensionless parameter l_0/r_N
β = dimensionless parameter y_0/r_N
γ = dimensionless parameter z_0/r_N
ρ = density
$\Delta\rho$ = absolute value of density difference between two phases
σ = interfacial tension

Subscripts

C = continuous phase
D = dispersed phase
f = conditions at final instant of drop separation
N = nozzle
0 = conditions at instant drop separation begins
s = static conditions

LITERATURE CITED

1. Batson, J. B., M.S. thesis, Univ. Tenn., Knoxville (1951).
2. Harkins, W. D., and F. E. Brown, *J. Am. Chem. Soc.*, **38**, 246 (1916).
3. *Ibid.*, **41**, 499 (1919).
4. Hayworth, C. B., and R. E. Treybal, *Ind. Eng. Chem.*, **42**, 1174 (1950).
5. Null, H. R., Ph.D. dissertation, Univ. Tenn., Knoxville (1955).
6. Null, H. R., M.S. thesis, Univ. Tenn., Knoxville (1951).

Manuscript received Sept. 5, 1956; revised Oct. 7, 1957; accepted Oct. 7, 1957.